A 3-D Organically Templated Mixed Valence (Fe^{2+}/Fe^{3+}) Iron Phosphate with Oxide-Centered $Fe_4O(PO_4)_4$ Cubes: Hydrothermal Synthesis, Crystal Structure, Magnetic Susceptibility, and Mössbauer Spectroscopy of $[H_3NCH_2CH_2NH_3]_2[Fe_4O(PO_4)_4]\cdot H_2O$

Jeffrey R. D. DeBord,[†] William M. Reiff,*[,‡] Christopher J. Warren,[†,⊥] Robert C. Haushalter,*[,†,⊥] and Jon Zubieta*[,§]

NEC Research Institute, 4 Independence Way, Princeton, New Jersey 08540, Department of Chemistry, Northeastern University, Boston, Massachusetts 02115, and Department of Chemistry, Syracuse University, Syracuse, New York 13244

Received March 3, 1997. Revised Manuscript Received June 5, 1997[⊗]

A 3-D, open framework, mixed valence iron phosphate, $[H_3NCH_2CH_2NH_3]_2[Fe_4O(PO_4)_4]\cdot H_2O$, which contains organic ethylenediammonium dications in the framework voids, has been prepared via hydrothermal synthesis and has been characterized by single-crystal X-ray diffraction, magnetic susceptibility, and variable temperature Mössbauer spectroscopy. Crystal data: tetragonal, space group $I\bar{4}2m$ with $a = 10.1383(8)$ Å, $c = 9.628(1)$ Å, $V = 989.6(1)$ Å^3, $Z = 2$, and $R(R_w) = 7.7(6.5)$ for 276 reflections ($I > 3\sigma(I)$) and 32 variables. The fundamental building block of the structure is a novel cubane-like cluster with trigonal bipyramidal iron and tetrahedral phosphorus atoms lying at alternate vertexes of a cube with a tetrahedrally coordinated oxygen atom at the center of the cube. Each cluster is linked by eight Fe−O−P bonds that extend along what would be all ⟨111⟩ directions of the putative cube to eight similar clusters to form a framework that is only slightly distorted (by the presence of the organic cations) from cubic $\bar{4}3m$ symmetry. Mössbauer and ac magnetic susceptibility measurements show that equal amounts of valence trapped Fe^{2+} and Fe^{3+} are present, which undergo long range magnetic ordering at ∼12 K.

Introduction

It has been recently shown that the incorporation of hydrogen-bonded organic molecules, especially diammonium cations, via hydrothermal synthesis is a very general method for the preparation of a large variety of novel organic−inorganic hybrid materials such as molybdenum phosphates,[1] vanadium phosphates,[2] vanadium phosphonates,[3] tin phosphonates,[4] cobalt phosphates,[5] indium phosphates,[6] and vanadium oxides.[7] This strategy has also been used to prepare the first organically templated layered Fe phosphate,[8] which was built up from phosphate-bridged 1-D strings of edge-sharing $Fe^{3+}O_6$ octahedra that order as a weak ferro-

[†] NEC Research Institute.
[‡] Northeastern University.
[§] Syracuse University.
[⊥] Current address: Symyx Technologies, 3100 Central Expy, Santa Clara, CA 95051.

[⊗] Abstract published in *Advance ACS Abstracts,* August 1, 1997.

(1) Haushalter, R.; Mundi, L. *Chem. Mater.* **1992**, *4*, 31.
(2) (a) Soghomonian, V.; Chen, Q.; Haushalter, R; Zubieta, J. *Chem. Mater.* **1993**, *5*, 1690. (b) Haushalter, R.; Wang, Z.; Thompson, M.; Zubieta, J.; O'Connor, C. *Inorg. Chem.* **1993**, *32*, 3966. (c) Soghomonian, V.; Chen, Q.; Haushalter, R.; Zubieta, J.; O'Connor, C. *Science* **1993**, *259*, 1596. (d) Soghomonian, V.; Chen, Q.; Haushalter, R.; Zubieta, J. *Chem. Mater.* **1993**, *5*, 1595. (e) Soghomonian, V.; Chen, Q.; Haushalter, R.; Zubieta, J. *Angew. Chem., Int. Ed. Engl.* **1993**, *32*, 610. (f) Haushalter, R.; Chen, Q.; Soghomonian, V.; Zubieta, J.; O'Connor, C. *J. Solid State Chem.* **1994**, *108*, 128. (g) Soghomonian, V.; Haushalter, R.; Zubieta, J. *Inorg. Chem.* **1994**, *33*, 3, 1700. (h) Zhang, Y.; Clearfield, A.; Haushalter, R. *J. Solid State Chem.* **1994**, *117*, 157. (i) Zhang, Y.; Clearfield, A.; Haushalter, R. *Chem. Mater.* **1995**, *7*, 1221. (j) Soghomonian, V.; Chen, Q.; Haushalter, R.; O'Connor, C.; Tao, C.; Zubieta, J. *Inog. Chem.* **1995**, *34*, 3509. (k) Khan, M.; Meyer, L.; Haushalter, R.; Zubieta, J.; Dye, J. *Chem. Mater.* **1996**, *8*, 43. (l) Soghomonian, V.; Haushalter, R.; Zubieta, J.; O'Connor, C. *Inorg. Chem.* **1996**, *35*, 2826. (m) Johnson, J. W.; Jacobson, A. J. *Angew. Chem., Int. Ed. Engl.* **1985**, *22*, 412. (n) Huan, G.; Jacobson, A. J.; Johnson, J. W.; Corcdan, E. W. *Chem. Mater.* **1990**, *2*, 91. (o) Riou, D.; Ferey, G. *Eur. J. Solid State Inorg. Chem.* **1994**, *31*, 25.
(3) (a) Kahn, M.; Lee, Y.; O'Connor, C.; Haushalter, R.; Zubieta, J. *J. Am. Chem. Soc.* **1994**, *116*, 4525. (b) Khan, M.; Lee, Y.; O'Connor, C.; Haushalter, R.; Zubieta, J. *Inorg. Chem.* **1994**, *33*, 3855. (c) Soghomonian, V.; Diaz, R.; Haushalter, R.; O'Connor, C.; Zubieta, J. *Inorg. Chem.* **1995**, *34*, 4460. (d) Soghomonian, V.; Haushalter, R.; Zubieta, J. *Chem. Mater.* **1995**, *7*, 1648. (e) Soghomonian, V.; Chen, Q.; Haushalter, R.; Zubieta, J. *Angew. Chem., Int. Ed. Engl.* **1995**, *34*, 223. (f) Bonavia, G.; Haushalter, R.; O'Connor, C.; Zubieta, J. *Inorg. Chem.* **1996**, *35*, 5603.
(4) Zapf, P.; Rose, D.; Haushalter, R.; Zubieta, J. *J. Solid State Chem.* **1996**, *125*, 182.
(5) (a) DeBord, J.; Haushalter, R.; Zubieta, J. *J. Solid State Chem.* **1996**, *125*, 270. (b) Chen, J.; Jones, R.; Natarajan, S.; Hursthouse, M.; Thomas, M. *Angew. Chem., Int. Ed. Engl.* **1994**, *33*, 639.
(6) Dhingra, S.; Haushalter, R. *J. Chem. Soc., Chem. Commun.* **1993**, *21*, 1665.
(7) (a) Zhang, Y.; O'Connor, C.; Clearfield, A.; Haushalter, R. *Chem. Mater.* **1996**, *8*, 595. (b) Zhang, Y.; DeBord, J.; O'Connor, C.; Haushalter, R.; Clearfield, A.; Zubieta, J. *Angew. Chem., Int. Ed. Engl.* **1996**, *35*, 989. (c) DeBord, J.; Zhang, Y.; Haushalter, R.; Zubieta, J.; O'Connor, C. *J. Solid State Chem.* **1996**, *122*, 251. (d) Zhang, Y.; Haushalter, R.; Clearfield, A. *J. Chem. Soc., Chem. Commun.* **1996**, *9*, 1055. (e) Zhang, Y.; Haushalter, R.; Clearfield, A. *Inorg. Chem.* **1996**, *35*, 4950. (f) Whittingham, M. S.; Guo, J. D.; Chen, R.; Chirayil, Th.; Janauer, G.; Zavalij, P. *Solid State Ionics*, **1995**, *75*, 257. (g) Duan, C. Y.; Tiang, Y. P.; Lu, Z. L.; You, Y. Z. *Inorg. Chem.* **1995**, *34*, 1. (h) Riou, D.; Ferey, G. *Inorg. Chem.* **1995**, *34*, 6520. (i) Pecharsky, V. P.; Jacobson, R. A. *Z. Kristallogr.* **1996**, 211. (j) Nazar, L. F.; Koene, B. E.; Britten, J. F. *Chem. Mater.* **1996**, *8*, 327.
(8) (a) Cavellec, M.; Riou, D.; Ferey, G. *Acta Crtstallogr.* **1995**, *C51*, 2242. (b) DeBord, J.; Reiff, W.; Haushalter, R.; Zubieta, J. *J. Solid State Chem.* **1996**, *125*, 186.
(9) (a) Moore, P.; Kampf, A. *Z. Kristallogr.* **1992**, *201*, 263. (b) Moore, P. *Am. Miner.* **1972**, *57*, 397. (c) Moore, P. *Am. Miner.* **1970**, *55*, 135. (d) Moore, P.; Araki, T. *Inorg. Chem.* **1976**, *15*, 316. (e) Moore, P. *The 2nd International Congress on Phosphorus Compounds Proceedings*, April 21−25, 1980; p 105. (f) Moore, P.; Shen, J. *Nature* **1983**, *306*, 356.

S0897-4756(97)00125-7 CCC: $14.00

magnetic state at 30 K. While there are a very large number of known iron phosphate minerals, characterized largely by Moore,[9] and many synthetic iron phosphates without entrained organic cations,[10] we are unaware of any 3-D iron phosphates containing organic templates. Several organically templated ferric fluorophosphates[11] do, however, exist. In this paper we describe the synthesis and structural characterization of $[H_3NCH_2CH_2NH_3]_2[Fe_4O(PO_4)_4]\cdot H_2O$, **1**, which contains a novel 3-D framework constructed from PO_4 tetrahedra and four FeO_5 trigonal bipyramids sharing a common vertex, and show through Mössbauer and ac magnetic susceptibility measurements that it contains equal amounts of valence trapped Fe^{2+} and Fe^{3+} that undergo magnetic ordering at ~12 K. While we are unaware of any known oxide-centered $Fe_4O(PO_4)_4$-type compounds, we note that oxide centered cubanes of the type $Ga_4F(PO_4)_4$ have been observed in the fluorinated gallophosphate cloverite and in the compound ULM-5.[12]

Experimental Section

Synthesis. Phosphate **1** is prepared in very low yield (~1%) from the hydrothermal treatment of finely divided Fe_2O_3, phosphoric acid, ethylenediamine, HF, and H_2O in the mole ratio of 1.0:7.6:8.9:3:444 for 90 h at 200 °C. The synthesis was carried out in a poly(tetrafluoroethylene)-lined stainless steel container under autogenous pressure. The 23 mL reaction vessel was filled to approximately 30% volume capacity, and all reactants were stirred briefly before heating. Phosphate **1** is isolated in the form of large, well-faceted, black prisms somewhat reminiscent of pentagonal dodecahedra. This preparation also gives crystals of the layered iron phosphate $[H_3NCH_2CH_2NH_3]_{0.5}[Fe(OH)(PO_4)]$,[8] and while many reaction variations have been attempted, the optimum reaction conditions for the preparation of **1** have not yet been discovered.

Magnetic Susceptibility. The ac magnetic susceptibility measurements were performed using a Lakeshore Cryogenics Series 7000 susceptometer applying an ac magnetic field of 1 Oe at a frequency of 125 Hz.

Mössbauer. Variable temperature Mössbauer spectra were recorded using equipment that was previously described.[13] α-Iron foil was employed as a standard. The spectra were fitted to Lorentzians, using a program written primarily by Stone.[14]

Crystallography. Although crystals of **1** appear to be visibly well-formed, we have found that most are unsuitable for single-crystal X-ray analysis. A black prism-shaped crystal of approximate dimensions 0.10 × 0.05 × 0.05 mm was mounted on a glass fiber. The X-ray and intensity data were collected on a Rigaku AFC7R four-circle diffractometer equipped with a 12 kW rotating anode generator using graphite monochromated Mo Kα radiation. Cell constants and an orientation matrix for data collection were obtained from the setting angles of 25 carefully centered reflections in the range $20.93° < 2\theta < 29.92°$ and corresponded to a body centered tetragonal cell with the unit cell dimensions given in Table 1. Although the data crystal indexed cleanly onto a body-centered tetragonal cell, the peaks were nevertheless quite broad.

Table 1. Crystallographic Data for $[H_3NCH_2CH_2NH_3]_2[Fe_4O(PO_4)_4]\cdot H_2O$[1]

empirical formula	$Fe_2P_2O_9C_2N2$
FW (g/mol)	369.67
crystal color, habit	black, prism
crystal dimensions (mm)	0.10 × 0.05 × 0.05
crystal system	tetragonal
space group	$I\bar{4}2m$ (no. 121)
lattice parameters	$a = 10.1383(8)$ Å $b = 9.628(1)$ Å $V = 989.6(1)$ Å^3
Z	2
D_{calc} (g·cm^{-3})	2.481
μ(Mo Kα)	32.93 cm^{-1}
scan type	$\omega-2\theta$
2θ max (deg)	60.1
total reflections	454
observed reflections ($I > 3.00\sigma(I)$)	276
no. of variables	32
reflection/parameter ratio	8.62
R; R_w	0.077; 0.065
goodness of fit	3.84
max/min peak in difference map (e$^-$/Å)	0.85/−0.90

The data collection consisted of scans of $(1.37 + 0.35 \tan\theta)°$ in the range $5° < 2\theta < 60.1°$, which were made at a speed of 16°/min (in ω). The weak reflections [$I < 20.0\sigma(I)$] were rescanned a maximum of four times. The intensities of three standard reflections were measured after every 150 reflections and over the course of data collection decreased in intensity by only 0.2%. A linear correction factor was applied to account for this phenomenon. An empirical correction using the program DIFABS[15] was also applied to the data and resulted in transmission factors ranging from 0.82 to 1.00. The data were also corrected for Lorentz and polarization effects.

The structure of **1** was solved by direct methods and refined on F by full-matrix least squares using the teXsan crystallographic software package of Molecular Structure Corporation.[16] The iron, phosphorus, and one of the oxygen atoms in the structure were refined with anisotropic temperature factors, but due primarily to a paucity of data, the remaining four oxygen atoms as well as the carbon and nitrogen atoms of the ethylenediamine molecule were refined isotropically. Hydrogen atoms were not included in the refinements. Carbon atom C[1] of the ethylenediammonium dication was found to be 2-fold disordered because of the symmetry elements of space group $I\bar{4}2m$. This atom lies on the Wyckoff 16*j* position resulting in two symmetry equivalent carbon atom positions, each position having an occupancy factor of 0.50. The disorder results in two possible conformations for the carbon atoms of the ethylenediammonium dication, both of which are depicted in Figure 2. The final least-squares refinement was based on 276 observed reflections [$I < 3.0\sigma(I)$] and 32 variable parameters and converged with $R(R_w) = 0.077(0.065)$. Further details of the structural analysis are given in Table 1, the final positional and equivalent isotropic thermal parameters are given in Table 2, and some important bond distances and angles are given in Table 3.

Results and Discussion

The structure of $[H_3NCH_2CH_2NH_3]_2[Fe_4O(PO_4)_4]\cdot H_2O$ **1** was solved in the body-centered tetragonal space group $I\bar{4}2m$ and consists of a three-dimensional framework composed of linked cubane-like iron phosphate clusters with ethylenediammonium cations and water molecules occupying the intercluster tunnels (Figure 1).

(10) (a) Lii, K.; Huang, C. *J. Chem. Soc., Dalton Trans.* **1995**, 571. (b) Gabelica-Robert, M.; Goreaud, M.; Labbe, Ph.; Raveau, B. *J. Solid State Chem.* **1982**, *45*, 389. (c) Pintard-Screpel, M.; D'Yvoire, F.; Durand, J. *Acta Crystallogr.* **1983**, *C39*, 9. (d) Riou, D.; Labbe, Ph.; Goreaud, M. *Eur. J. Solid State Inorg. Chem.* **1988**, *25*, 215. (e) Reiff, W.; Torardi, C. *Hyperfine Interact.* **1990**, *53*, 403.

(11) (a) Cavellec, M.; Riou, D.; Ninclaus, C.; Greneche, J.; Ferey, G. *Zeolites* **1996**, *17*, 250. (b) Cavellec, M.; Riou, D.; Greneche, J. M.; Ferey, G. *J. Magn. Mater.* **1996**, *163*, 173. (c) Cavellec, M.; Riou, D.; Greneche, J. M.; Ferey, G. *Microporous Mater.* **1997**, *8*, 3.

(12) (a) Estermann, M.; McCusker, L. B.; Merrouche, A.; Kessler, H. *Nature* **1991**, *352*, 320. (b) Linde, A.; Simmen, A.; Patrin, J.; Baerlocher, C. *Proceedings of the 9th International Zeolite Conference*, Montreal; Von Balmoos, R., et al., Eds.; 1992; p 433. (c) Loiseau, T.; Ferey, G. *J. Solid State Chem.* **1994**, *111*, 403.

(13) Chang, C.; Reiff, W. *Inorg. Chem.* **1977**, *16*, 2097.

(14) Bancroft, G.; Maddock, A.; Ong, W.; Prince, R.; Stone, A. *J. Chem. Soc. A* **1967**, 1966.

(15) Walker, N.; Stuart, D. *Acta Crystallogr.* **1983**, *A39*, *158*.

(16) *teXsan Single-Crystal Structure Analysis Software Package*, Version 1.7−1; Molecular Structure Corporation: The Woodlands, TX, 1995.

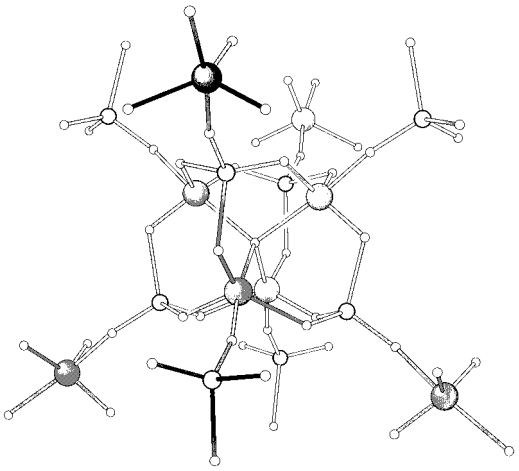

Figure 1. View of the "Fe_4P_4" oxo cluster in **1**. The Fe, P, and O atoms are represented by spheres of decreasing size.

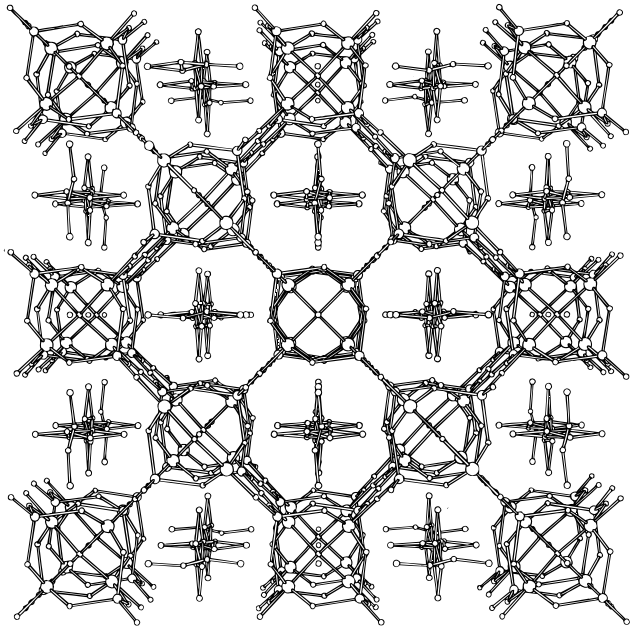

Figure 2. Unit cell view of the structure of $[H_3NCH_2CH_2NH_3]_2[Fe_4O(PO_4)_4]\cdot H_2O$ **1** down the crystallographic *c* axis.

Table 2. Atomic Coordinates and Temperature Factors (B_{Eq}) for $[H_3NCH_2CH_2NH_3]_2[Fe_4O(PO_4)_4]\cdot H_2O$ (1)

atom	*x*	*y*	*z*	B_{eq}[a]
Fe(1)	0.3736(2)	0.3736(2)	0.1212(4)	3.04(3)
P(1)	0.1689(4)	0.1689(4)	0.3039(8)	3.60(8)
O(1)	0.299(1)	0.524(2)	0.223(1)	5.7(3)
O(2)	0.5000	0.5000	0.0000	4.5(8)
O(3)	0.296(1)	0.2961()	−0.052(2)	5.3(5)
O(4)	0.254(2)	0.254(2)	0.190(3)	7.6(6)
O(5)	0.0000	0.0000	0.0000	6.5(7)
N(1)	0.185(2)	0.5000	0.5000	3.8(4)
C(1)	0.045(2)	0.490(3)	0.561(2)	1.7(4)

[a] $B_{eq} = 8/3\pi^2(U_{11}(aa^*)^2 + U_{22}(bb^*)^2 + U_{33}(cc^*)^2 + 2U_{12}aa^*bb^* \cos\gamma + 2U_{13}aa^*cc^* \cos\beta + 2U_{23}bb^*cc^* \cos\alpha)$.

The basic building block of the framework is the novel "Fe_4P_4" oxo cluster, which is shown in Figure 2. The cluster contains four trigonal bipyramidal iron centers, each sharing a common vertex that is a μ^4-tetrahedrally coordinated oxygen atom residing in the center of the cube. The four remaining vertexes of the cube are occupied by tetrahedrally coordinated phosphorus atoms. Oxygen atoms very approximately occupy the midpoints of the cube edge and form Fe−O−P bonds.

Table 3. Selected Bond Lengths (Å) and Angles (deg) for $[H_3NCH_2CH_2NH_3]_2[Fe_4O(PO_4)_4]\cdot H_2O$ (1)

bond lengths		bond angles	
Fe(1)−O(1)	1.97(2)[a]	O(1)−Fe(1)−O(1)	110.3(8)
Fe(1)−O(2)	2.156(3)	O(1)−Fe(1)−(O2)	92.2(4)
Fe(1)−O(3)	2.00(2)	O(1)−Fe(1)−(O3)	124.7(4)
Fe(1)−O(4)	1.84(3)	O(1)−Fe(1)−O(4)	94.5(6)
P(1)−O(1)	1.53(2)[a]	O(2)−Fe(1)−O(3)	90.9(6)
P(1)−O(3)	1.47(2)	O(2)−Fe(1)−O(4)	168.3(8)
P(1)−O(4)	1.64(3)	O(3)−Fe(1)−O(4)	77.4(9)
		Fe(1)−O(2)−Fe(1)	107.04(9)
		Fe(1)−O(2)−Fe(1)	114.5(2)
		Fe(1)−O(1)−P(1)	125.3(9)
		Fe(1)−O(3)−P(1)	126(1)
		Fe(1)−O(4)−P(1)	159(1)

[a] Atoms Fe(1) and P(1) are bonded to two symmetry equivalent oxygen atoms.

Hence, except for the four Fe−O bonds emanating from the central μ^4 oxygen atom, there are only Fe−O−P bonds within the structure of **1**.

The 3-D network structure observed in **1** is constructed by linking the "Fe_4P_4" oxo clusters together into a solid through the eight corners of the aforementioned cube to eight neighboring crystallographically equivalent Fe_4P_4 cubes via the Fe−O−P bonds that run parallel to the body diagonals of the cube. Accordingly, each exopolyhedral Fe−O bond is connected to a phosphorus atom of a neighboring cube, while the similar P−O bonds coordinated to the iron atoms are likewise bonded to phosphorus atoms belonging to the other four neighboring cubes.

In principle, if undistorted, the framework structure of **1** would possess cubic $I\bar{4}3m$ symmetry. As observed, however, the framework of **1** has undergone a slight compression along what is the tetragonal [001] direction because of the noncubic distribution of the organic cations and water solvate. This distortion, although small (*a*/*c* ratio is ca. 1.053), has an effect on the structure of **1**, forcing the organic cations to be 2-fold disordered from the $I\bar{4}2m$ symmetry constraints. As in many of our other organically templated oxides, the ammonium cations are strongly H-bonded to the O atoms of the framework, and for this example have N···O distances in the range of 3.05−3.22 Å.

The iron sites in $[H_3NCH_2CH_2NH_3]_2[Fe_4O(PO_4)_4]\cdot H_2O$ (**1**) are mixed valence Fe^{2+}/Fe^{3+}. If one assumes that the organic cation possesses a charge of 2+, then the average oxidation state of the iron in **1** is formally 2.5+. However, since the iron atom lies on the Wyckoff 8*i* position in $I\bar{4}2m$, all of the iron atoms in the structure of **1** are *crystallographically* equivalent. Valence sum calculations[17] done on the structure of **1** show the Fe atom to possess an oxidation state of 2.7+. Normally, one would expect to see different Fe−O bond lengths associated with the 2+ and 3+ oxidation states, but here they are forced to be equivalent because of the space group symmetry. However, we speculate that the difference in bond lengths expected from the presence of both Fe^{2+} and Fe^{3+} shows up in the abnormally broad peak widths in the X-ray diffraction pattern of **1**, which have an average peak width of 0.32° (in ω). Such a large peak width could be due to the superposition of many unit cells, each possessing a different ordering of the

(17) Brown, I. *Structure and Bonding in Crystals*; O'Keeffe, M., Navrotsky, A., Eds.; Academic Press: New York, 1981; Vol. II.

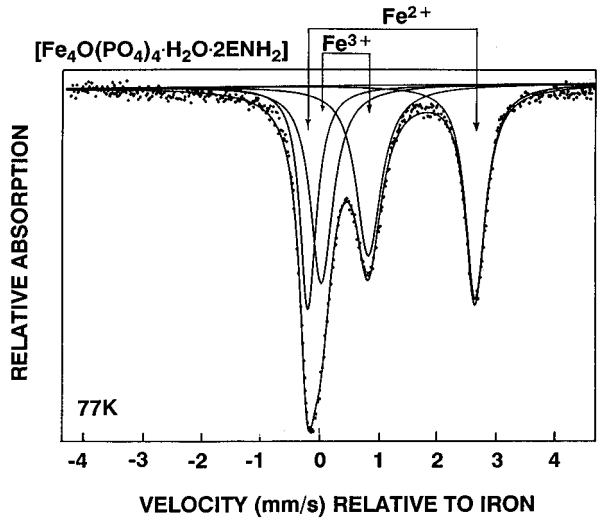

Figure 3. Mössbauer spectrum of **1** at 77 K showing the overlap of two quadrupole doublets typical of high-spin iron 2^+ and high-spin iron 3^+.

Fe^{2+}/Fe^{3+} sites with a given tetrahedron relative to the tetrahedra in neighboring cells, thus giving rise to slight random distortions in all six lattice directions. Therefore, the random superposition of the slightly different cells might give rise to the observed broad peaks.

The trapped, mixed valence nature of the Fe in **1** has been confirmed by Mössbauer spectroscopy measurements at 77 K, as shown in Figure 3, for a mosaic of hand-picked crystals. Herein one observes the overlap of two quadrupole doublets typical of high-spin iron 2+ and high-spin iron 3+.[18] In particular, the corresponding isomer shifts (δ) (relative to natural iron foil) and quadrupole splittings (ΔE) are: $\delta(Fe^{2+}) = 1.22$ mm/s, $\Delta E(Fe^{2+}) = 2.84$ mm/s and $\delta(Fe^{3+}) = 0.43$ mm/s, $\Delta E(Fe^{3+}) = 0.80$ mm/s. The intensity ratio ($I_{Fe}{}^{2+}/I_{Fe}{}^{3+}$) is 0.90, which is consistent with an expected somewhat higher recoil-free fraction for the ferric sites. The spectrum at ambient temperature is very similar to that at 77 K, giving no evidence of incipient valence detrapping behavior. It should be noted that the line widths for the transitions of Figure 3 range from ~0.35 to ~0.50 mm/s. Such broadening is consistent with Fe^{2+}/Fe^{3+} disorder in view of the fact that the normal line widths of thin absorbers on our spectrometer are ~0.25 mm/s.

The temperature dependence of the Mössbauer spectrum of **1** is shown in Figure 4 at a higher overall velocity sweep for a polycrystalline powder sample. Here, a weak magnetic hyperfine impurity background corresponding to an α-Fe_2O_3 impurity (used in the synthesis) is apparent (see arrows in the 77 K spectrum). Below about 12 K, magnetic hyperfine splitting signaling the onset of cooperative long range magnetic ordering of **1** occurs, and the expected multiple overlapping hyperfine patterns are evident with magnetic saturation below 2 K.

The underlying nature of the magnetic behavior of **1** is suggested from the temperature dependence of its magnetic moment as determined from ac susceptibility measurements. In particular, the effective magnetic moment of **1** is only ~8 μ_B/mol (4 μ_B/Fe) at ambient temperature versus 10.86 μ_B/mol (5.43 μ_B/Fe) theoretically expected for spin only behavior and noninteracting metal atoms in the Fe_4P_4 oxo-centered cluster. As seen in Figure 5, the evident antiferromagnetic exchange leads to a further gradual but steady decrease in moment (μ/Fe ~ 3.7 μ_B at 78 K to μ/Fe ~ 3.4 μ_B at ~15 K). Below ~12 K and coincident with the 3-D ordering suggested by the Mössbauer spectra, there is an abrupt further decrease in μ to ~1.8 μ_B at 4.2 K. The strong out-of-phase component, χ'', of the magnetic susceptibil-

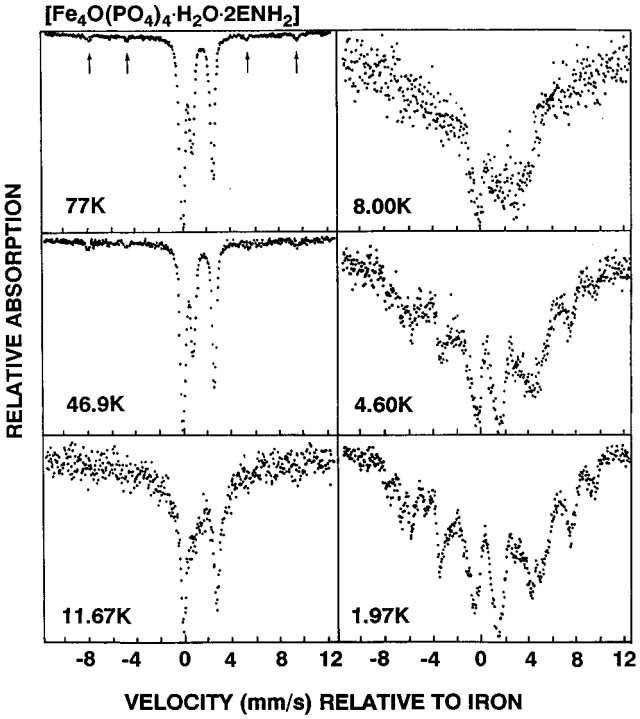

Figure 4. Temperature dependence of the Mössbauer spectrum for a polycrystalline powder sample of **1**. The weak magnetic hyperfine impurity background corresponding to α-Fe_2O_3 is apparent at 77 K (arrows).

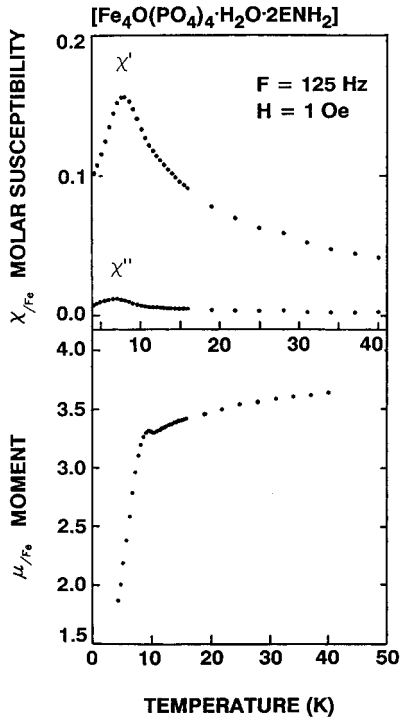

Figure 5. Ac susceptibility measurements and the temperature dependence of the magnetic moment of **1**.

(18) Greenwood, N.; Gibb, T. *Mössbauer Spectroscopy*; Chapman and Hall: London, 1982.

ity below ~12 K indicates a 3-D magnetically ordered ground state with a net magnetic moment, namely ferrimagnetism or canted antiferromagnetism. The choice between these two possibilities awaits further detailed study, preferably by single-crystal magnetization studies or by neutron diffraction. In any event, one reasonable qualitative scenario for the overall temperature dependence of χ_m and μ_{eff} is simple intracluster AF-exchange, but with intercluster AF-exchange dominating at lower temperatures such that 3-D order occurs at $T_N \sim 12$ K among the "remaining" thermally unquenched moments of the clusters. The behavior of **1** is similar in a number of aspects to that of $FeAsO_4$.[19] This material contains antiferromagnetically coupled 5-coordinate Fe^{III} dimer pairs that undergo long range order ($T_N \sim 68$ K) at lower temperature owing to interdimer exchange interactions.

In passing, we note that the trace of α-Fe_2O_3 present in the sample of **1** is not expected to influence our interpretation of the susceptibility data for **1**. This material is strongly antiferromagnetic[20] ($T_N \sim 950$ K) with very weak canting that disappears below ~260 K, the Morin transition.[18]

(19) Reiff, W.; Kwiecien, M.; Jakeman, R.; Cheetham, A.; Torardi, C. *J. Solid State Chem*. **1993**, *107*, 401.

(20) Cullity, B. *Introduction to Magnetic Materials*; Addison-Wesley: Reading, MA, 1972.

These results demonstrate the applicability of hydrothermal syntheses for the preparation of hybrid organic–inorganic materials, which has now been extended to include the 3-D iron phosphate system. On the basis of the very large number of synthetic, and especially mineral, examples of iron phosphate framework solids, our results suggest that the organically templated materials will be a fertile area for synthesis in the future.

Acknowledgment. The work at Syracuse University was supported by NSF Grant CHE9617232. J.Z. also acknowledges the donors of the Petroleum Research Fund, administered by the American Chemical Society, for support of the research at Syracuse under Grant PRF 30651-ACS5, 3. W.M.R. acknowledges the NSF Division of Materials Research for funds for the ac susceptometer.

Supporting Information Available: Experimental details, tables of atomic coordinates, anisotropic displacement parameters, bond lengths and angles, and nonbonded contacts (12 pages); observed and calculated structure factors for **1** (3 pages). Ordering information is given on any curreny masthead page.

CM970125B